Thickness Dependence of the Young's Modulus of Polymer Thin Films

Jooyoung Chang¹, Kamil B. Toga^{1†}, Joseph D. Paulsen^{1,2,3}, Narayanan Menon², Thomas P. Russell^{1*}

¹Department of Polymer Science and Engineering, University of Massachusetts,

Amherst, MA 01003

²Department of Physics, University of Massachusetts, Amherst, MA 01003

³Department of Physics and Soft and Living Matter Program, Syracuse University,

Syracuse, NY 13244

[†]Current address: Avomeen Analytical Services, Ann Arbor, MI 48108

AUTHOR INFORMATION

Corresponding Authors

*E-mail: russell@mail.pse.umass.edu

ABSTRACT

The Young's modulus of polymer thin films was measured from bulk films that are microns in thickness down to films having a thickness of \sim 6 nm, which is less than the radius of gyration, R_g . A single, non-invasive technique in a single geometry, i.e. the wrinkling of a free-floating film on a water surface with a droplet of water on the surface of the film, was used to determine the modulus over this very large range of film thicknesses. Unlike a solid substrate there are no in-plane stresses exerted on the film by the underlying liquid substrate except at the boundary of the film. Using recent theoretical developments in the treatment of wrinkling phenomena, we extracted the film modulus from measurements of the wrinkle length. The Young's modulus does not show any systematic change with film thickness, from the thickest bulk films down to films with a thickness of $\sim R_g$ for both PS and PMMA, although a slight increase of the Young's modulus was found for the thinnest sub- R_g thick PS film.

INTRODUCTION

As the size of devices and manufactured structures continues to shrink, the mechanical properties of thin polymer films, an integral component of many flexible devices, become increasingly important. The demands for the accurate characterization of mechanical behavior of solution-processed films have grown, since novel data obtained from delicate structures are applicable to the state-of-the-art technologies, for example organic semi-conductors, solar cell devices, coatings, and photoresists. However, whether the static and dynamic properties change as the thickness of polymer films approaches molecular dimensions or less, is still an open question. There have been numerous reports on the glass transition temperature (T_g) as a function of film thickness, as measured by a variety of techniques. 1,2,11-20,3,21-30,4,31-35,5-10 Each of these techniques measures a specific property of the film as a function of temperature, under a range of experimental conditions. Films have been supported on hard and soft elastic substrates where interfacial interactions have been varied, or they have been suspended in air and supported at the edges by a hard substrate. Studies of polymer films floated on different liquid substrates with freely standing conditions have also been conducted to determine the properties of Tg, elastic modulus, compliance, strain, viscosity, and viscoelastic dewetting. 11,26,36-40 Films have also been prepared using a range of different conditions, including solution-casting and thermal annealing. A broad spectrum of results have emerged with some reports of significant changes in Tg as a function of film thickness, arising primarily from interfacial (substrate and air) effects that propagate into the film, while others report little change in the properties of the thin films.

Here, we present measurements of the mechanical properties of PS and PMMA films that are prepared by spin-coating and are freely floating on the surface of water. Unlike a solid substrate, a fluid substrate exerts a uniform in-plane stress only at the boundary of the film. We

studied the wrinkling of a free floating circular film on a water surface with a droplet of water placed on the center of the film. The wavelength and length of the wrinkles were used to determine the modulus of polystyrene and poly(methylmethacrylate) thin films. 41,42,43 The thickness of the films was varied over 2 orders of magnitude, for PS (from 6.8 nm to 993.3 nm), and PMMA (from 7.2 nm to 545.1 nm) where the molecular weights of the polymers were $\sim 10^5$ g/mol. Consequently, the film thicknesses varied from $\sim R_g/2$ to $\sim 100~R_g$, i.e. from submolecular to the bulk. The Young's modulus did not change with thickness over the large range of film thicknesses we used in our experiment.

EXPERIMENTAL SECTION

PS (M_w = 97 Kg/mol, M_w/M_n = 1.06, R_g ~ 10 nm, and T_g = 100°C) was purchased from Polymer Source. PMMA (M_w = 99.6 Kg/mol, Rg ~ 9 nm, T_g = 115°C, and syndio:hetero:iso content was 55:37:8) was purchased from Sigma-Aldrich. Both PS and PMMA were used as received. The molecular weights of both polymers were selected to be higher than the critical entanglement molecular weight (PS: 35 Kg/mol, PMMA: 29.5 Kg/mol).^{44, 45, 46} PS and PMMA were dissolved in toluene (Anhydrous, 99.8%, Sigma-Aldrich) and anisole (Anhydrous, 99.8%, Sigma-Aldrich), respectively.

To produce smooth, uniform films with the desired thicknesses and minimal defects, spin coating was used. Polymer solutions were spin-coated onto 3 cm \times 3 cm pre-cut polished silicon wafers with a native oxide layer (2 nm), using spinning speeds from 1000 to 9000 RPM for 60 seconds. The silicon wafer substrates were pre-cleaned using a carbon dioxide snow-jet cleaner and UV-Ozone treatment (JElight, Model No.342) for 15 minutes. The solutions were filtered through a 0.2 μ m Whatman PTFE filter directly onto the substrate to remove dust and other

impurities. By varying the concentrations of the solution (from 0.6 wt% to 10 wt%) and the spinning speed, a wide range of thicknesses of films was obtained for both PS (6.8 nm ~ 993 nm) and PMMA (7.2 nm ~ 545.1 nm). PMMA films were spin-coated in a relative humidity of less than 20%. The films were dried at ambient conditions to fully remove solvent.

The spin-coated films were then cut into discs of varying diameters (W = 15 mm to 45 mm), using a tungsten carbide cutting tool and floated onto the surface of water. A small water droplet (0.3 μ l) was initially placed at the center of the floating sheet with a glass microsyringe. Wrinkle patterns were formed rapidly, with the number and length of wrinkles determined in tens of milliseconds after the water droplet was applied.⁴² The volume of water was increased in 0.2 μ l increments from 0.2 \sim 0.3 μ l until the total volume of the water droplet was between 0.9 and 1.1 μ l. The resulting wrinkle pattern generated by the drop was captured with an optical profilometer (Zygo) and a stereo microscope (Olympus SZ 40) equipped with a digital camera (Nikon D7100). These images were analyzed using ImageJ and Matlab to determine the number and the length of the wrinkles with high precision. To measure the thickness, the floating films were retrieved with a silicon wafer, dried completely under vacuum at room temperature, and the thickness was measured with an interferometer (Filmetrics F20-UV) with a resolution of 1 nm. Scanning probe microscopy was used to confirm these measurements.

Figure 1 (a-d) shows wrinkle patterns for 669.3 and 6.8 nm thick PS films, and 533 and 16.3 nm thick PMMA films floating on the surface of water after placing water droplets at the center of the films. For both PS and PMMA, decreasing the thickness, t, leads to an increase in the number and a decrease in the length of the wrinkles, consistent with previous studies.^{41–43} When the sheet is placed on the surface of water, it experiences a radial tensile stress at the boundary due to the air-water surface tension (γ), and is thus everywhere in tension. When a drop

is placed on the sheet, it exerts a different radial tension at the 3-phase contact line at the edge of the drop. The leads to a region of compressive hoop stress ($\sigma_{\theta\theta}$ < 0) around the drop. If this exceeds the critical compressive stress threshold for buckling in the azimuthal direction, wrinkles form in a region a < r < a + L in which a is a radius of a drop and L is the length of wrinkles. For the thickness range of our films, we are far above this threshold, and the formation of wrinkles erases the compressive stress in the wrinkled region. Relevant theoretical calculations for this so-called far-from-threshold regime have been presented elsewhere.

As we will describe in the next section, the length, L, of the wrinkles depends on the liquid-vapor surface tension (γ), the contact angle of the drop, and the stretching modulus, Y= Et, where E is Young's modulus and t is the thickness of a film.^{43,47} The number, N, of the wrinkles depends on the elastic properties of the film through the bending modulus, $B = \text{Et}^3/12(1-\Lambda^2)$ where Λ is the Poisson ratio. Given the film thickness, we can thus determine the Young's modulus, E, of the film from two different measurements of the number of wrinkles or their length in different films. The length of wrinkles is more sensitive to the Young's modulus than the number of wrinkles.

Figure 1 (a-d)

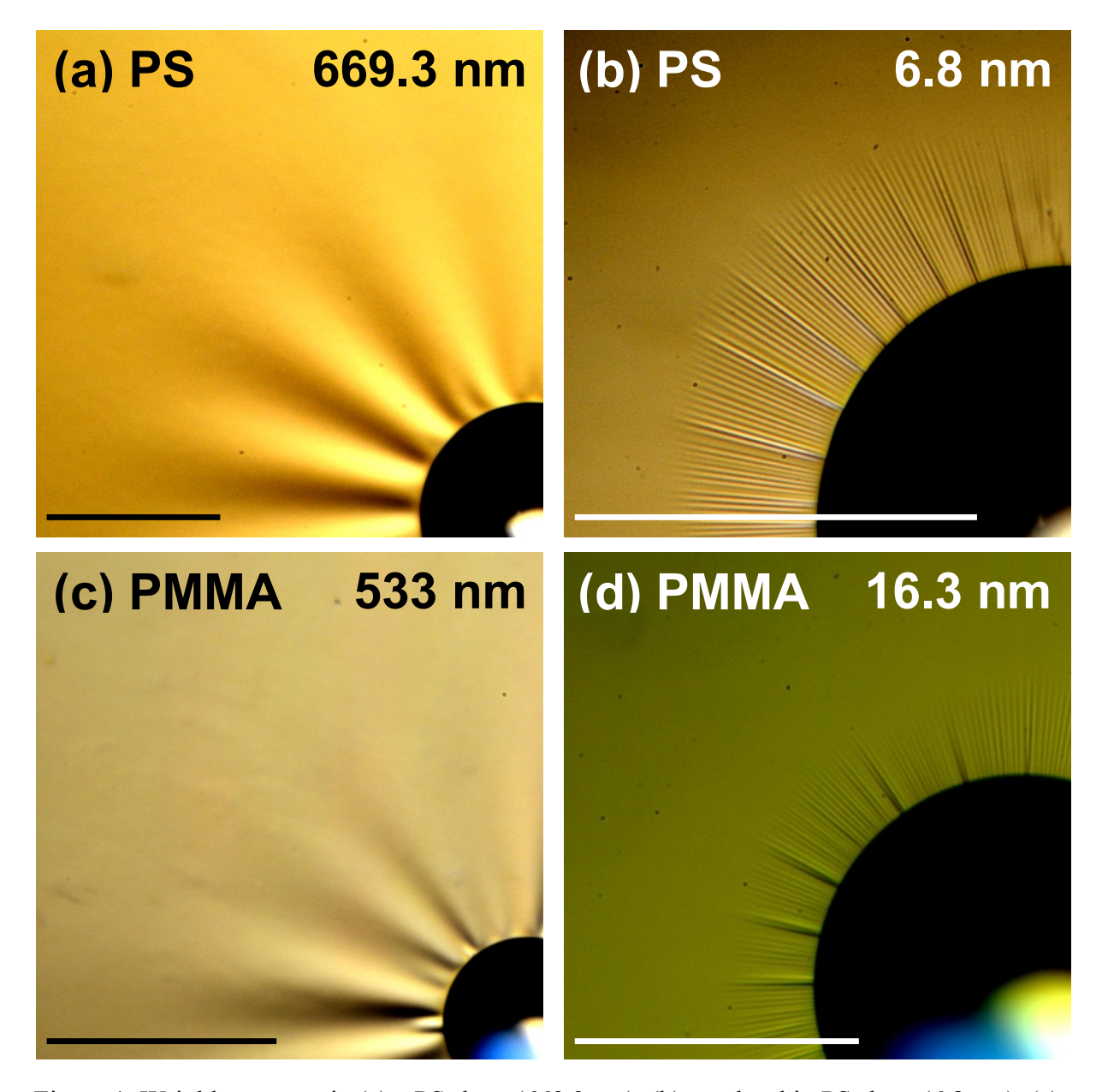


Figure 1. Wrinkle patterns in (a) a PS sheet (669.3 nm), (b) an ultrathin PS sheet (6.8 nm), (c) a PMMA sheet (533 nm), and (d) an ultrathin PMMA sheet (16.3 nm). Droplet volumes in (a-d) are 0.9, 0.7, 0.5 and 0.7 μ L, respectively. Lengths of scale bars are 1 mm.

DATA ANALYSIS

 Estimation of the length of wrinkles using a Far From Threshold (FT) analysis of the wrinkling instability.⁵⁰ Recent theoretical work has provided the relationship between L and the experimental parameters in the far-from-threshold (FT) regime of the wrinkling instability. ^{43,47} In that work, the Lamé solution for an annulus under different tensile radial stresses was used to calculate stress components in radial (σ_{rr}) and hoop ($\sigma_{\Theta\Theta}$) directions to estimate the length of the wrinkles:

$$L = \frac{\tau a}{2} \qquad (a < r < a + L) (1)$$

$$\tau \approx \frac{\gamma}{\gamma_{hath}} \left(\frac{3}{10} \frac{\sin^2 \theta}{x \ln x}\right)^{\frac{1}{3}} \quad (2)$$

where γ is the surface tension of the water drop, γ_{bath} is the surface tension of the water medium supporting the floated polymer film, θ is the contact angle of the liquid drop with the thin film, and $x = (\gamma/\text{Et})$. The confinement parameter, τ , is defined as $\tau \equiv \frac{\sigma_{rr}(^o)}{\gamma}$ where $\sigma_{rr}(^o)$ is the 2D radial stress outside of the contact line between water droplet and the film. $^{41,50-52}$ Equations (1) and (2) were used with $x = (\gamma/\text{Et})$ to calculate the solid line shown in Figure 2(a) and 3(a) where $E_{PS} = 5.9$ GPa, 6.8 nm $\leq t_{PS} \leq 993$ nm, $\gamma = \gamma_{bath} = 72$ mN/m, and $\theta_{PS} = 88^o$ for water on PS in Figure 2(a) and $E_{PMMA} = 4.6$ GPa, $7.2 \leq t_{PMMA} \leq 545.1$ nm, $\gamma = \gamma_{bath} = 72$ mN/m, and $\theta_{PMMA} = 68^o$ for water on PMMA in Figure 3(a). Young's moduli of PS and PMMA, E_{PS} and E_{PMMA} , as a function of film thickness, t, were calculated applying equations (1) and (2) with t = t in Figure 2(c) and 3(c), using the Nsolve function in Mathematica to solve for the value of the Young's modulus, with the same values for the other system parameters as reported above. Here, the t values for PS and PMMA were obtained using image analysis with Matlab.

2. Estimation of the number of wrinkles by the local λ law.⁵⁰

When the dominant source for the stiffness against wrinkling is the tension in the film, then a recent theoretical treatment, which we call the local λ law, ⁴⁹ predicts for the number of wrinkles:

$$N(r) \approx \left(\frac{\tau \gamma_{bath} ar}{4B}\right)^{1/4} \left| \frac{\log(L/r) - 1}{\log(L/r)} \right|^{1/2} (3)$$

where r is the radial distance, τ is the confinement parameter expressed in equation (2), a is the radius of a droplet, B is the bending modulus, and L is the length of the wrinkle determined using the confinement parameter, τ . If this formula is modified to include stiffness due to the gravitational cost of deforming the water substrate, then:

$$N(r) \approx r \left[\frac{\rho g + \left(\frac{\tau \gamma_{bath} a}{4r^3}\right) \left(\frac{\log(L/r) - 1}{\log(L/r)}\right)^2}{B} \right]^{1/4}$$
(4)

where the density of water, $\rho = 1000 \text{ kg/m}^3$ and gravitational acceleration, $g = 9.81 \text{ m/s}^2$. This formula depends on radial position; we evaluate it at r = (a+L)/2, that is at half the length of the wrinkle. We note that the theory is approximate, in that it does not address the elastic boundary layers at the contact line and the wrinkle tip (r = a and r = L) as we discuss later. Furthermore, the tension is not uniform in the radial direction, but these formulae make the first approximation of using the local value of tension rather than including terms that explicitly involve the spatial gradient of the stiffness. To obtain the lines in Figure 2(b) and 3(b), the parameters, a = 1 mm, $E_{PS} = 3.4 \text{ GPa}$, $E_{PMMA} = 3.0 \text{ GPa}$, $E_{$

RESULTS AND DISCUSSION

To measure wrinkle lengths, images of the wrinkle patterns were obtained by two different methods (stereo microscopy and optical profilometry), and were analyzed using Matlab

to extract the wrinkle lengths. Normalized wrinkle profiles, $\zeta(r)$, determined as a function of the normalized wrinkle lengths by the two methods, are shown in Figure S1. The lengths track each other as the variables (thickness, material, drop radius) are changed, but the values of L measured by the optical profilometer were consistently $\sim 10\%$ larger than those determined by stereo microscopy (Figure S2).

Figures 2(a), 2(b) and 2(c) show the thickness dependence of the length of wrinkles (L), the number of wrinkles (N), and the calculated Young's modulus for PS. Three different diameters (W = 15, 23, and 45 mm) were investigated to eliminate artifacts arising from the finite size of the sheets in comparison to the wrinkle length. The data from the three sets did not differ significantly. The thickness of the PS films ranged from 6.8 to 993.3 nm, i.e. from sub-R_g in thickness to effectively bulk values. The solid line in Figure 2(a) shows the predicted wrinkle length (L/a) as a function of the film thickness (t), calculated using equations (1) and (2) with E_{PS} = 5.9 GPa. This trend of the stiffening in glassy polymer films is also suggested by Page et al., Tweedie et al., and O'Connell et al. $^{20,53-55}$ The deviation of the calculated Young's modulus, E_{PS} = 5.9 GPa, from the bulk modulus of PS, E_{PS}=3.4 GPa, may be due to two subtle physical effects not included in the calculation. The first is that the wrinkles do not end sharply at a point. A boundary layer where the wrinkle tip meets the flat part of the wrinkle is ignored.⁴⁷ Second. the boundary conditions at the contact line, where the wrinkles meet the edge of the droplet, are complex and not easily modelled.⁴² We do not expect these systematic effects to influence the determination of the thickness dependence of the modulus.

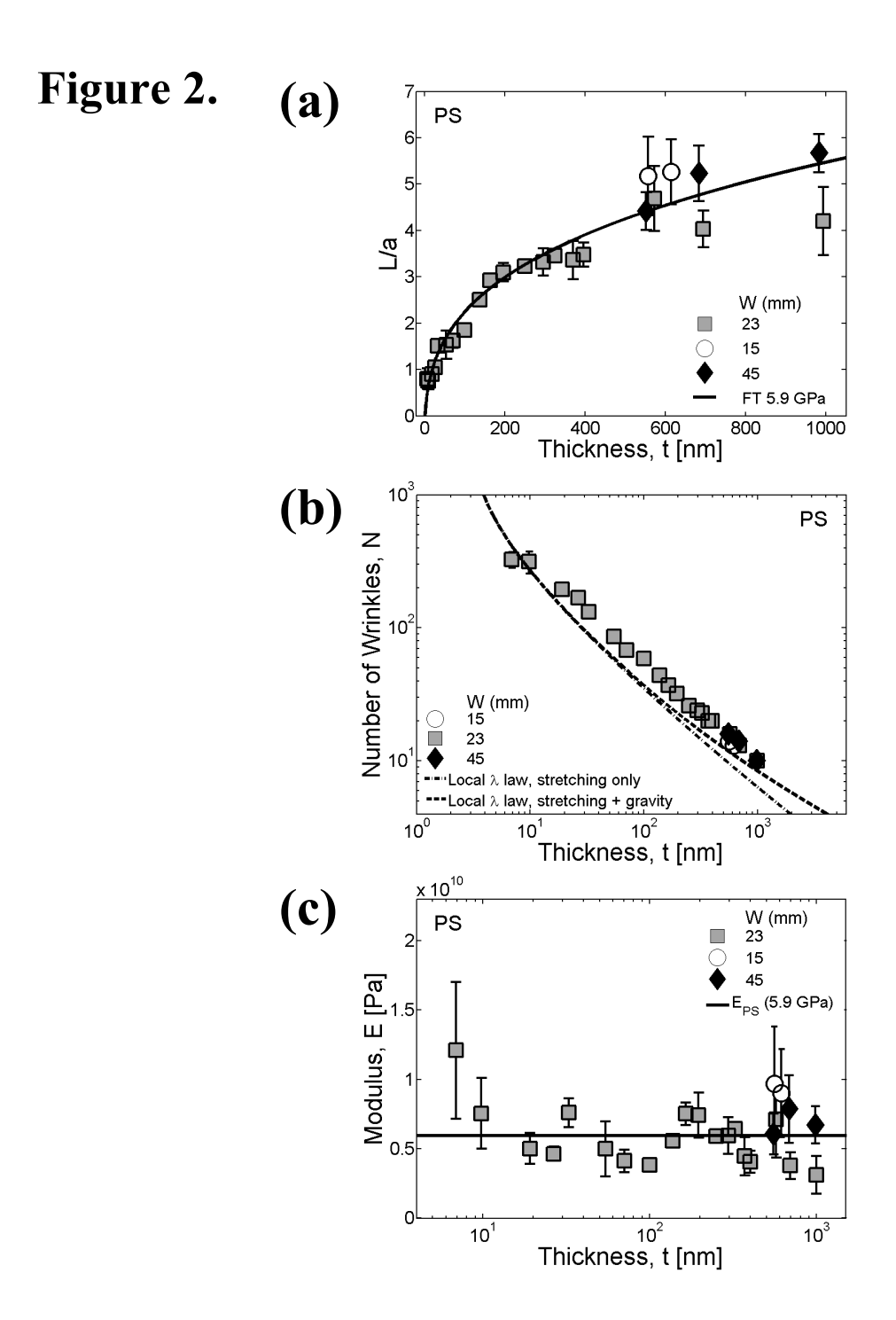


Figure 2. (a) Normalized length of wrinkles (L/a) versus thickness of PS. A solid line is obtained from equation (1). (b) Number of wrinkles (N) versus thickness of PS. A dashdotted line is obtained from an equation (3) and a dashed line is obtained from an equation (4). (c) Young's moduli of PS (E_{ps}) obtained via the length of wrinkles versus thickness of PS, measured by solving equation (1) for E_{ps}.

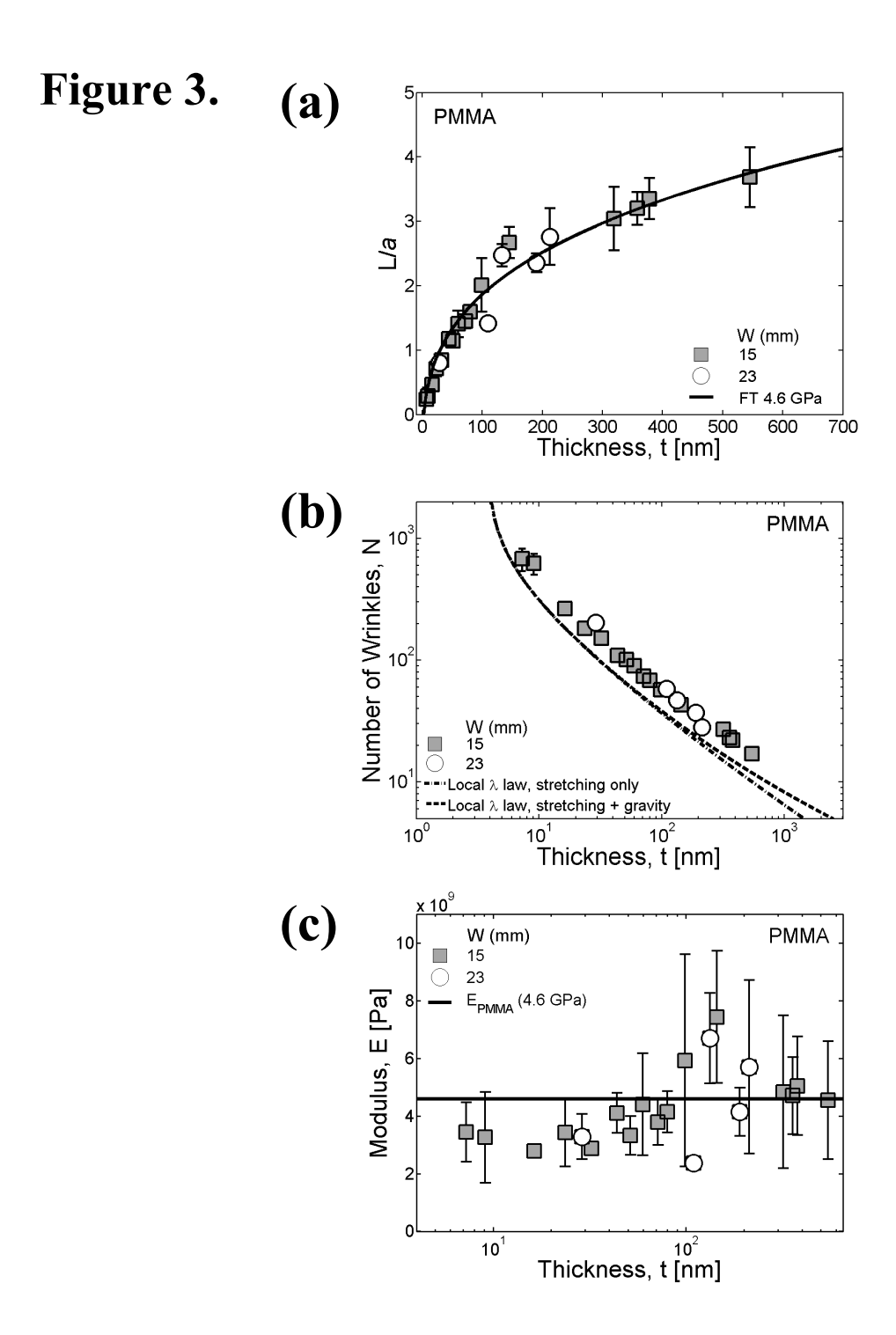


Figure 3. (a) Normalized length of wrinkles (L/a) versus thickness of PMMA. A solid line is obtained from equation (1). (b) Number of wrinkles (N) versus thickness of PMMA. A dashdotted line is obtained from an equation (3), and a dashed line is obtained from an equation (4). (c) Young's moduli of PMMA (E_{pmma}) obtained by the length of wrinkles versus thickness of PMMA, measured by solving equation (1) for E_{pmma} .

The results from the wrinkle patterns and the Young's Modulus obtained for free-floating films of PMMA sheets are shown in Figure 3(a), 3(b) and 3(c). The thickness of the films range from 7.2 nm to 545.1 nm with two different sheet diameters (W = 15 mm and 23 mm) being used to detect edge and finite size effects. Similar to the results for PS films, the normalized length (L/a) versus thickness (t) results for the free-floating PMMA films, over the entire thickness range investigated, could be described using equation (1) and (2) in Figure 3(a), with a modulus of 4.6 GPa. This departs from the bulk value of the Young's modulus of PMMA, $E_{PMMA} = 3.0$ GPa. Here too, the physical effects described above are not included in the calculation.

The number of wrinkles, N, as a function of film thickness, t, for PS and PMMA are exhibited in Figure 2(b) and 3(b), respectively. Here, we plot the theoretical predictions using the bulk values of the Young's moduli for these materials ($E_{PS} = 3.4$ GPa and $E_{PMMA} = 3.0$ GPa, respectively). The data are consistent with no change in the Young's modulus as a function of t, as shown by the comparison with equation (3) and (4) for calculating the N versus t in Figure 2(b) and 3(b). The underestimations of the local λ law shown in both Figure 2(b) and 3(b) patterns might be caused by the existence of non-negligible gradients in the substrate stiffness, or the ignored boundary layers at the unclear wrinkle end (r = L) and contact line between the water droplet and the polymer film (r = a), which could be significantly varied depending on the thickness of the polymer films, as seen in Figure 5.

Using equations (1) and (2), the thickness dependence of Young's moduli of PS and PMMA was calculated in Figure 2(c) and 3(c), respectively. As can be seen, over the broad range of film thicknesses investigated from sub- R_g to the bulk, the values of Young's modulus, E, estimated from the wrinkle length, L, do not show a systematic dependence on film thickness for PS and PMMA, with at most a slight increase at the smallest thicknesses in the case of PS. We

will return to these observations, and place them in the context of other data. It is important to note that the wrinkle pattern measured from the PMMA films floated on water for an hour did not change with time, indicating that the adsorbed water did not affect the wrinkle patterns or the Young's moduli inferred from these data.

For both PS and PMMA thin films, polymers with bulk glass transitions temperatures of 100°C and 115°C, respectively, the Young's moduli of the polymers as a function of film thickness determined from the wrinkle patterns (Figure 2(c) and 3(c)) are in agreement with the bulk values of these polymers in the glassy state. These results indicate that the glass transition temperature of the thin films, even for films that are less than R_{g} in thickness, must be much higher than the measurement temperature. It is remarkable that this holds even for films thin enough that the polymer chains must be compressed in the direction normal to the film surface. Previous studies have shown that, in the plane of the film, the R_{g} of the polymer is the same as that in the bulk.⁵⁶ The volume pervaded by a single chain is $V_p = A < R_g^2 >^{3/2} = A'(M/m)^{3/2}b^3$ where M is the molecular weight of the polymer, m is the monomer molecular weight, b is the size of a segment and A and A' are constants. The occupied volume of the chain is given by $V_0=(M/m)V_s$, where V_s is the segment volume. The entanglement molecular weight is defined by the molecular weight where V_o/V_p is constant. When the thin films are under strong confinement, less than R_g, and if we assume that the average shape of the volume pervaded by the polymer chain is an oblate ellipsoid in the thin films, then for films of thickness $\sim R_g/2$, the entanglement molecular weight is doubled, approaching the molecular weight of the polymers used in this study. The results from these wrinkling experiments show only a slight increase in the Young's modulus for very thin PS films. For PMMA, no indication of a change in the modulus is observed. If there is a slight increase in the modulus for PS at ambient temperature, this

indication of stiffer ultrathin polymer films would agree with Page et al. Tweedie et al, and O'Connell et al.^{20,53–55} Page et al. established a composite model with experimental results, showing the stiffening effect of polymer films when the thickness of the film is less than $5 \sim 10$ R_g, Tweedie et al. argued that the apparent stiffness increases up to 200% as the contact depth (h_c) of an indentation probe, which induces a hydrostatic pressure under the probe, decreases less than 20 nm using nanoindentation measurement, while O'Connell et al. reported that the glassy compliances of 4.2 nm and 9.1 nm of polycarbonate films and 11.3 nm and 17.1 nm of a polystyrene film were stiffened $2 \sim 2.5$ times in freestanding states with the bubble inflation method.^{20,53–55} The arguments proposed by, Page et al., Tweedie et al. and O'Connell et al., however, would not be expected to apply here, since there is no composite, solid substrate, or high deformation rate. While the total number of chains contacting the interfaces does not increase with decreasing film thickness, there is an increased probability that individual chains span across the film and have multiple contacts with the interfaces. With an increase in the entanglement molecular weight (based on V₀/V_p) due to confinement, a stiffening of the confined polymer chain or an increase in the Young's modulus for ultrathin films is understandable. It is even more striking that no change in the modulus was observed for PMMA films close to and less than R_g in thickness.

Figure 4.

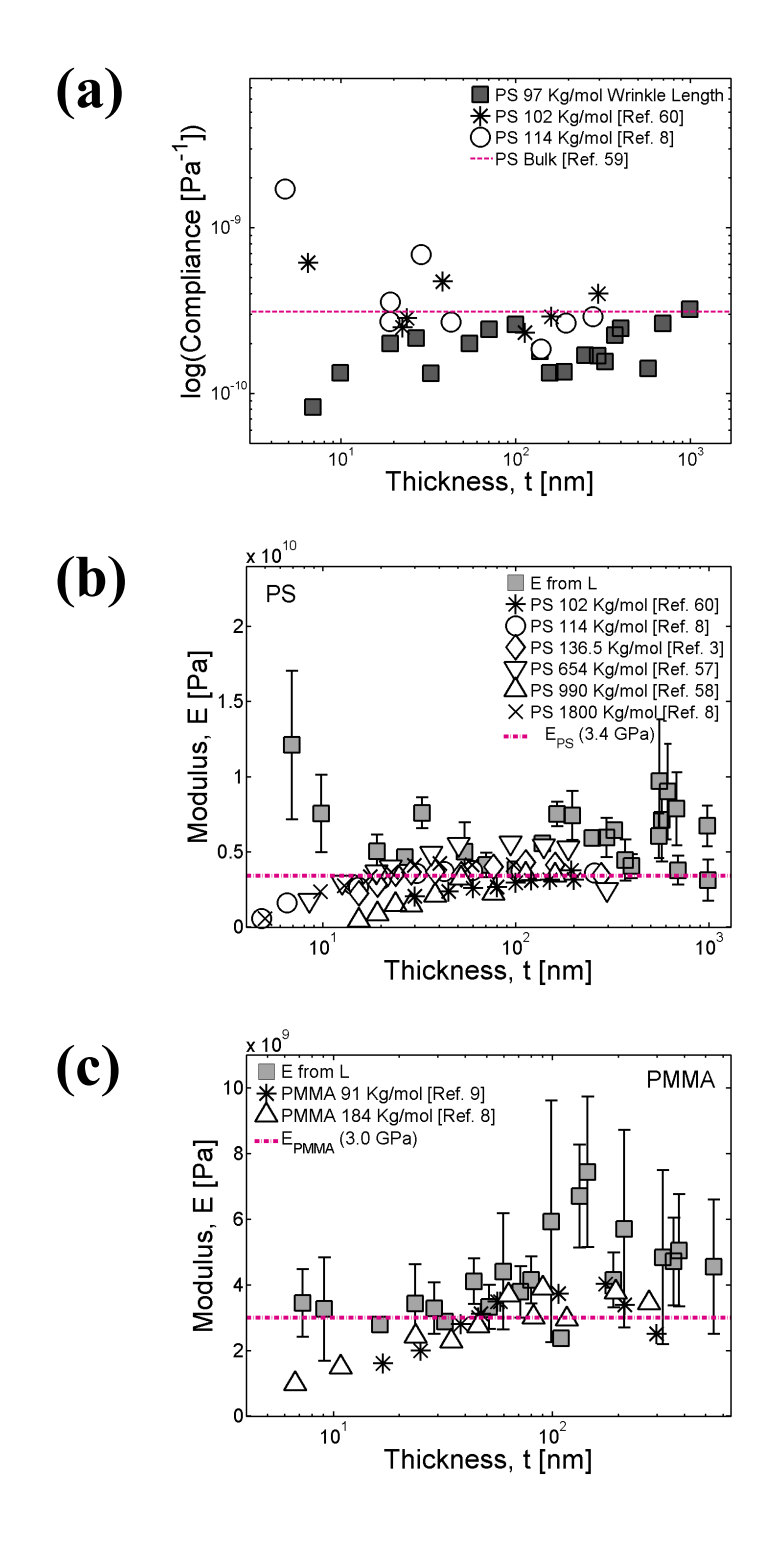


Figure 4. (a) Compliance of PS versus thickness, (b) Young's moduli of PS (E_{ps}) versus thickness, and (c) Young's moduli of PMMA (E_{pmma}) versus thickness.

We also calculated the compliance for thin films of PS and PMMA from the modulus, and compared these to results in the literature 11,16,17,57,58,59,60 as shown in Figure 4(a), 4(b), and 4(c), respectively. To directly compare the data to bulk PS compliance results obtained by Plazek, all the literature and the experimental data obtained were converted from the Young's modulus to the compliance in Figure 4.59 As can be seen, the compliance data obtained from the wrinkle experiments, for PS and PMMA films with thicknesses from less than 10 nm up to the bulk, are similar to the glassy uniaxial compliance results, D, converted from the shear compliance value, J = 3D, for bulk PS by Plazek, ~ 3.1 × 10⁻¹⁰ Pa⁻¹ (indicated by dashed line). ^{54,59,61} The Young's moduli data determined by the length of wrinkles from both PS and PMMA, on the other hand, show clear deviations from the literature. This indicates that the Young's modulus of PS increases when the thickness of PS film is $\sim R_g \, (\text{Figure 4(b)})$ and the Young's modulus of PMMA does not change (Figure 4(c)) as opposed to the data from the literature which indicate a decrease of Young's moduli when the thickness of PS and PMMA is less than 25 nm or greater. 11,16,60 We argue that the gentle nature of the capillary force induced wrinkling, i.e. $\sigma_{max}=$ $\sigma(r=a) = \tau \gamma/t \sim (\gamma/t)^{2/3} E^{1/3} \sim 38 \text{ MPa},^{43} \text{ may contribute to these differences, since the}$ polymer film becomes extremely brittle with a decrease in the film thicknesses (~ R_g) at a point where the effective entanglement molecular weight starts to increase.^{35,62} Page et al. also observed similar phenomena under small strains ($\varepsilon \le 5\%$) with PFSA membranes but our data do not agree with their model, which suggests that an increase in E occurs for a thickness from 5 $\sim 10~R_{\rm g}.^{20}$

In addition to the simple wrinkling behavior, different classes of wrinkle patterns were observed over different ranges in the film thickness. Figure 5 shows the different classes of wrinkle patterns. Two Fourier modes, i.e. two different frequencies with different amplitudes

were observed for films having thicknesses $t \le \sim 50$ nm. A cascade of wrinkles wavelengths at the contact line with the water droplet was observed for films with thicknesses 50 nm $\le t \le 600$ nm. A single mode, one wrinkle wavelength with single amplitude, was observed for films with thicknesses $t \ge 600$ nm. The number, amplitude, and length of the different wrinkle patterns varied with changes in the film thicknesses. These different modes of wrinkling may arise from changes in the bending rigidity of the film at the water contact line as the thickness is varied. At present, we do not have a quantitative description of the origin of these different classes of wrinkle patterns.

CONCLUSION

We measured the number and the length of wrinkles generated by capillary forces in films of PS and PMMA. From these data we extracted the mechanical properties for film thicknesses ranging from sub- R_g to the bulk. The mechanical properties for both PS and PMMA were found to be independent of thickness down to ~ 10 nm, though, for the thinnest sub- R_g thick PS film, a slight increase in the modulus was observed. We also found the existence of different classes of wrinkle patterns: a single mode, a double mode, and a cascading of wrinkles in the vicinity of the contact line between the water droplet and the floating films.

Figure 5.

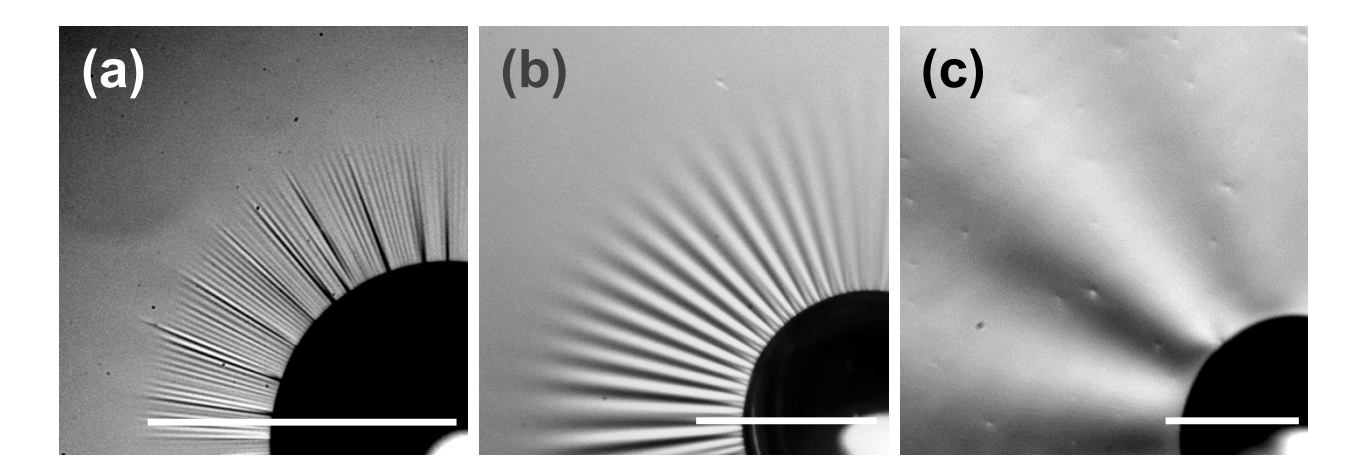


Figure 5. Optical micrographs of three different classes of wrinkle patterns on PS: (a) Two fourier mode (thickness of a PS film (t) \leq 50 nm), (b) Single mode with 2N cascades (50 nm \leq t \leq 600 nm), and (c) Single mode (t \geq 600 nm). Lengths of scale bars are 1 mm.

ASSOCIATED CONTENTS

Supporting Information

Supporting Information: Figures S1-S3 and Supplementary Text (PDF)

Notes

The authors declare no competing financial interest.

ACKNOWLEDGEMENTS

This work was supported by the W.M. Keck Foundation, NSF-DMR-1507650, and NSF-

DMR-CAREER-1654102. We thank B. Davidovitch, D. Kumar, M. Byun, J.H. Na, S. Chantarak,

J. Choi, J. Patel, S. Kim, D.M. Yu, H. Kim, S. Srivastava, Z. Fink, and H. W. Wang for fruitful

discussions.

REFERENCES

(1) O'Connell, P. A.; McKenna, G. B. Rheological Measurements of the Thermoviscoelastic

Response of Ultrathin Polymer Films. Science 2005, 307, 1760–1763.

(2) O'Connell, P. A.; Mckenna, G. B. A Novel Nano-Bubble Inflation Method for

Determining the Viscoelastic Properties of Ultrathin Polymer Films. Scanning 2008, 30,

184–196.

(3) Sun, L.; Dutcher, J. R.; Giovannini, L.; Nizzoli, F.; Stevens, J. R.; Ord, J. L. Elastic and

Elasto-Optic Properties of Thin Films of Poly(Styrene) Spin Coated onto Si(001). J. Appl.

Phys. 1994, 75, 7482–7488.

20

- (4) Forrest, J. A.; Veress, K. D.; Dutcher, J. R. Brillouin Light Scattering Studies of the Mechanical Properties of Thin Freely Standing Polystyrene Films. *Phys. Rev. E* **1998**, *58*, 6109–6114.
- (5) Sharp, J. S.; Forrest, J. A. Dielectric and Ellipsometric Studies of the Dynamics in Thin Films of Isotactic Poly(Methylmethacrylate) with One Free Surface. *Phys. Rev. E* **2003**, 67, 9.
- (6) Every, A. G. Measurement of the Near-Surface Elastic Properties of Solids and Thin Supported Films. *Meas. Sci. Technol.* **2002**, *13*, R21–R39.
- (7) Zhao, J. H.; Kiene, M.; Hu, C.; Ho, P. S. Thermal Stress and Glass Transition of Ultrathin Polystyrene Films. *Appl. Phys. Lett.* **2000**, *77*, 2843–2845.
- (8) Jones, R.; Kumar, S.; Ho, D.; Briber, R.; Russell, T. Chain Conformation in Ultrathin Polymer Films. *Nature* **1999**, *400*, 146–149.
- (9) Jones, R. L.; Kumar, S. K.; Ho, D. L.; Briber, R. M.; Russell, T. P. Chain Conformation in Ultrathin Polymer Films Using Small-Angle Neutron Scattering. *Macromolecules* **2001**, *34*, 559–567.
- (10) Kerle, T.; Lin, Z.; Kim, H.; Russell, T. P. Mobility of Polymers at the Air / Polymer Interface. *Macromolecules* **2001**, *34*, 3484–3492.
- (11) Liu, Y.; Chen, Y. C.; Hutchens, S.; Lawrence, J.; Emrick, T.; Crosby, A. J. Directly Measuring the Complete Stress-Strain Response of Ultrathin Polymer Films.

 *Macromolecules** 2015, 48, 6534–6540.

- (12) Liu, Y.; Russell, T. P.; Samant, M. G.; Stöhr, J.; Brown, H. R.; Cossy-Favre, A.; Diaz, J. Surface Relaxations in Polymers. *Macromolecules* **1997**, *30*, 7768–7771.
- (13) DeMaggio, G.; Frieze, W.; Gidley, D.; Zhu, M.; Hristov, H.; Yee, a. Interface and Surface Effects on the Glass Transition in Thin Polystyrene Films. *Phys. Rev. Lett.* **1997**, 78, 1524–1527.
- (14) Bowden, N.; Brittain, S.; Evans, A. G.; Hutchinson, J. W.; Whitesides, G. M. Spontaneous Formation of Ordered Structures in Thin Films of Metals Supported on an Elastomeric Polymer. *Nature* **1998**, *393*, 146–149.
- (15) Stafford, C. M.; Harrison, C.; Beers, K. L.; Karim, A.; Amis, E. J.; VanLandingham, M. R.; Kim, H.-C.; Volksen, W.; Miller, R. D.; Simonyi, E. E. A Buckling-Based Metrology for Measuring the Elastic Moduli of Polymeric Thin Films. *Nat. Mater.* 2004, *3*, 545–550.
- (16) Stafford, C. M.; Vogt, B. D.; Harrison, C.; Julthongpiput, D.; Huang, R. Elastic Moduli of Ultrathin Amorphous Polymer Films. *Macromolecules* **2006**, *39*, 5095–5099.
- (17) Torres, J. M.; Stafford, C. M.; Vogt, B. D. Elastic Modulus of Amorphous Polymer Thin Films: Relationship to the Glass Transition Temperature. *ACS Nano* **2009**, *3*, 2677–2685.
- (18) Böhme, T. R.; de Pablo, J. J. Evidence for Size-Dependent Mechanical Properties from Simulations of Nanoscopic Polymeric Structures. *J. Chem. Phys.* **2002**, *116*, 9939–9951.
- (19) Van Workum, K.; de Pablo, J. J. Computer Simulation of the Mechanical Nanostructures.

 Nano Lett. 2003, 3, 1405–1410.

- (20) Page, K. A.; Kusoglu, A.; Stafford, C. M.; Kim, S.; Kline, R. J.; Weber, A. Z. Confinement-Driven Increase in Ionomer Thin-Film Modulus. *Nano Lett.* **2014**, *14*, 2299–2304.
- (21) Ellison, C. J.; Torkelson, J. M. The Distribution of Glass-Transition Temperatures in Nanoscopically Confined Glass Formers. *Nat. Mater.* **2003**, *2*, 695–700.
- (22) Priestley, R. D.; Ellison, C. J.; Broadbelt, L. J.; Torkelson, J. M. Structural Relaxation of Polymer Glasses at Surfaces, Interfaces, and in Between. *Science* **2005**, *309*, 456–459.
- (23) Mansfield, K. F.; Theodorou, D. N. Atomistic Simulation of a Glassy Polymer Surface. *Macromolecules* **1990**, *23*, 4430–4445.
- (24) Alcoutlabi, M.; McKenna, G. B. Effects of Confinement on Material Behaviour at the Nanometre Size Scale. *J. Phys. Condens. Matter* **2005**, *17*, R461–R524.
- (25) Keddie, J.L.; Jones, R.A.L.; Cory, R. A.; Size-Dependent Depression of the Glass Transition Temperature in Polymer Films. *Europhys. Lett.* **1994**, *27*, 59–64.
- (26) Lu, H.; Chen, W.; Russell, T. P. Relaxation of Thin Films of Polystyrene Floating on Ionic Liquid Surface. *Macromolecules* **2009**, *42*, 9111–9117.
- (27) Lee, H.; Paeng, K.; Stephen F. Swallen, M. D. E. Direct Measurement of Molecular Mobility in Actively Deformed Polymer Glasses. *Science* **2009**, *323*, 231–234.
- (28) Paeng, K.; Ediger, M. D. Molecular Motion in Free-Standing Thin Films of Poly(Methyl Methacrylate), Poly(4-Tert-Butylstyrene), Poly(α-Methylstyrene), and Poly(2-Vinylpyridine). *Macromolecules* **2011**, *44*, 7034–7042.

- (29) Paeng, K.; Swallen, S. F.; Ediger, M. D. Direct Measurement of Molecular Motion in Freestanding Polystyrene Thin Films. *J. Am. Chem. Soc.* **2011**, *133*, 8444–8447.
- (30) Tanaka, K.; Taura, A.; Ge, S.-R.; Takahara, A.; Kajiyama, T. Molecular Weight Dependence of Surface Dynamic Viscoelastic Properties for the Monodisperse Polystyrene Film. *Macromolecules* **1996**, *29*, 3040–3042.
- (31) Kajiyama, T.; Tanaka, K.; Takahara, A. Surface Molecular Motion of the Monodisperse Polystyrene Films. *Macromolecules* **1997**, *9297*, 280–285.
- (32) Tsui, O. K. C.; Wang, X. P.; Ho, J. Y. L.; Ng, T. K.; Xiao, X. Studying Surface Glass-to-Rubber Transition Using Atomic Force Microscopic Adhesion Measurements.

 *Macromolecules** 2000, 33, 4198–4204.
- (33) Wallace, W. E.; Van Zanten, J. H.; Wu, W. L. Influence of an Impenetrable Interface on a Polymer Glass-Transition Temperature. *Phys. Rev. E* **1995**, *52*, R3329–R3332.
- (34) Tress, M.; Mapesa, E. U.; Kossack, W.; Kipnusu, W. K.; Reiche, M.; Kremer, F. Glassy Dynamics in Condensed Isolated Polymer Chains. *Science* **2013**, *341*, 1371–1374.
- (35) Brown, H. R.; Russell, T. P. Entanglements at Polymer Surfaces and Interfaces. *Macromoelcules* 1996, 29, 798–800.
- (36) Bodiguel, H.; Fretigny, C. Reduced Viscosity in Thin Polymer Films. *Phys. Rev. Lett.* **2006**, *97*, 1–4.
- (37) Bodiguel, H.; Fretigny, C. Viscoelastic Dewetting of a Polymer Film on a Liquid Substrate. *Eur. Phys. J. E* **2006**, *19*, 185–193.

- (38) Bodiguel, H.; Fretigny, C. Viscoelastic Properties of Ultrathin Polystyrene Films. *Macromolecules* **2007**, *40*, 7291–7298.
- (39) Wang, J.; McKenna, G. B. Viscoelastic and Glass Transition Properties of Ultrathin Polystyrene Films by Dewetting from Liquid Glycerol. *Macromolecules* **2013**, *46*, 2485–2495.
- (40) Wang, J.; McKenna, G. B. Viscoelastic Properties of Ultrathin Polycarbonate Films by Liquid Dewetting. *J. Polym. Sci. Part B Polym. Phys.* **2015**, *53*, 1559–1566.
- (41) Huang, J.; Juszkiewicz, M.; de Jeu, W. H.; Cerda, E.; Emrick, T.; Menon, N.; Russell, T.P. Capillary Wrinkling of Floating Thin Polymer Films. *Science* 2007, *317*, 650–653.
- (42) Toga, K. B.; Huang, J.; Cunningham, K.; Russell, T. P.; Menon, N. A Drop on a Floating Sheet: Boundary Conditions, Topography and Formation of Wrinkles. *Soft Matter* **2013**, *9*, 8289–8296.
- (43) Schroll, R. D.; Adda-Bedia, M.; Cerda, E.; Huang, J.; Menon, N.; Russell, T. P.; Toga, K.
 B.; Vella, D.; Davidovitch, B. Capillary Deformations of Bendable Films. *Phys. Rev. Lett.*2013, 111, 1–5.
- (44) Majeste, J. C.; Montfort, J. P.; Allal, A.; Marin, G. Viscoelasticity of Low Molecular Weight Polymers and the Transition to the Entangled Regime. *Rheol. Acta* **1998**, *37*, 486–499.
- (45) Fetters, L. J.; Lohse, D. J.; Colby, R. H. CHAPTER 25 Chain Dimensions and Entanglement Spacings. *Phys. Prop. Polym. Handb.* **2006**, 445–452.

- (46) Fuchs, K.; Friedrich, C.; Weese, J. Viscoelastic Properties of Narrow-Distribution Poly (Methyl Methacrylates). *Macromolecules* **1996**, *9297*, 5893–5901.
- (47) Davidovitch, B.; Schroll, R. D.; Vella, D.; Adda-Bedia, M.; Cerda, E. a. Prototypical Model for Tensional Wrinkling in Thin Sheets. *Proc. Natl. Acad. Sci.* **2011**, *108*, 18227–18232.
- (48) King, H.; Schroll, R. D.; Davidovitch, B.; Menon, N. Elastic Sheet on a Liquid Drop Reveals Wrinkling and Crumpling as Distinct Symmetry-Breaking Instabilities. *Proc. Natl. Acad. Sci.* **2012**, *109*, 9716–9720.
- (49) Paulsen, J. D.; Hohlfeld, E.; King, H.; Huang, J.; Qiu, Z.; Russell, T. P.; Menon, N.; Vella, D.; Davidovitch, B. Curvature-Induced Stiffness and the Spatial Variation of Wavelength in Wrinkled Sheets. *Proc. Natl. Acad. Sci.* 2016, 113, 1144–1149.
- (50) Schroll, R. D.; Adda-Bedia, M.; Cerda, E.; Huang, J.; Menon, N.; Russell, T. P.; Toga, K.
 B.; Vella, D.; Davidovitch, B. Capillary Deformations of Bendable Films. *Phys. Rev. Lett.*2013, 111, 1–12.
- (51) Timoshenko, S.; Goodier, J. N. *Theory of Elasticity*, 3rd ed.; McGraw-Hil: New York, 1969.
- (52) Toga, K. B.; Huang, J.; Cunningham, K.; Russell, T. P.; Menon, N. A Drop on a Floating Sheet: Boundary Conditions, Topography and Formation of Wrinkles. *Soft Matter* **2013**, *9*, 8289.

- (53) Tweedie, C. A.; Constantinides, G.; Lehman, K. E.; Brill, D. J.; Blackman, G. S.; Van Vliet, K. J. Enhanced Stiffness of Amorphous Polymer Surfaces under Confinement of Localized Contact Loads. *Adv. Mater.* **2007**, *19*, 2540–2546.
- (54) O'Connell, P. A.; Hutcheson, S. A.; McKenna, G. B. Creep Behavior of Ultra-Thin Polymer Films. *J. Polym. Sci. Part B Polym. Phys.* **2008**, *46*, 1952–1965.
- (55) O'Connell, P. A.; Wang, J.; Ishola, T. A.; McKenna, G. B. Exceptional Property Changes in Ultrathin Films of Polycarbonate: Glass Temperature, Rubbery Stiffening, and Flow. *Macromolecules* **2012**, *45*, 2453–2459.
- (56) Hall, C. *Polymer Materials: An Introduction for Technologists and Scientists*; Macmillan Education LTD: London, 1989; Vol. 2.
- (57) Lee, J. H.; Chung, J. Y.; Stafford, C. M. Effect of Confinement on Stiffness and Fracture of Thin Amorphous Polymer Films. *ACS Macro Lett.* **2012**, *1*, 122–126.
- (58) Torres, J. M.; Stafford, C. M.; Vogt, B. D. Impact of Molecular Mass on the Elastic Modulus of Thin Polystyrene Films. *Polymer* **2010**, *51*, 4211–4217.
- (59) Plazek, D. J. Temperature Dependence of the Viscoelastic Behavior of Polystyrene. *J. Phys. Chem.* **1965**, *69*, 3480–3487.
- (60) Maillard, D.; Kumar, S. K.; Fragneaud, B.; Kysar, J. W.; Rungta, A.; Benicewicz, B. C.; Deng, H.; Brinson, L. C.; Douglas, J. F. Mechanical Properties of Thin Glassy Polymer Films Filled with Spherical Polymer-Grafted Nanoparticles. *Nano Lett.* 2012, *12*, 3909–3914.
- (61) Ferry, J. D. Viscoelastic Properties of Polymers, 3rd ed.; Wiley: New York, 1980.

(62) Si, L.; Massa, M. V.; Dalnoki-Veress, K.; Brown, H. R.; Jones, R. A. L. Chain Entanglement in Thin Freestanding Polymer Films. *Phys. Rev. Lett.* **2005**, *94*, 1–4.

For Table of Contents Use Only

